The 3'-untranslated region of XB130 regulates its mRNA stability and translational efficiency in non-small cell lung cancer cells

QINRONG WANG[1,2*], LINGLING LIU[1,2*], XUANJING GOU[1,2], TING ZHANG[1,2], YAN ZHAO[1,2], YUAN XIE[1,2], JIANJIANG ZHOU[1,2], YING LIU[1,2] and KEWEI SONG[1-3]

[1]Key Laboratory of Endemic and Ethnic Diseases, Ministry of Education; [2]Key Laboratory of Medical Molecular Biology, School of Basic Medicine; [3]Department of Sport and Health, Guizhou Medical University, Guiyang, Guizhou 550004, P.R. China

Received April 7, 2023; Accepted August 2, 2023

DOI: 10.3892/ol.2023.14013

Abstract. Silencing XB130 inhibits cell proliferation and epithelial-mesenchymal transition in non-small cell lung cancer (NSCLC), suggesting that downregulating XB130 expression may impede NSCLC progression. However, the molecular mechanism underlying the regulation of XB130 expression remains unclear. In the present study, the role of the 3'-untranslated region (3'-UTR) in the regulation of XB130 expression was investigated. Recombinant psiCHECK-2 vectors with wild-type, truncated, or mutant XB130 3'-UTR were constructed, and the effects of these insertions on reporter gene expression were examined using a dual-luciferase reporter assay and reverse transcription-quantitative PCR. Additionally, candidate proteins that regulated XB130 expression by binding to critical regions of the XB130 3'-UTR were screened for using an RNA pull-down assay, followed by mass spectrometry and western blotting. The results revealed that insertion of the entire XB130 3'-UTR (1,218 bp) enhanced reporter gene expression. Positive regulatory elements were primarily found in nucleotides 113-989 of the 3'-UTR, while negative regulatory elements were found in the 1-112 and 990-1,218 regions of the 3'-UTR. Deletion analyses identified nucleotides 113-230 and 503-660 of the 3'-UTR as two major fragments that likely promote XB130 expression by increasing mRNA stability and translation rate. Additionally, a U-rich element in the 970-1,053 region of the 3'-UTR was identified as a negative regulatory element that inhibited XB130 expression by suppressing translation. Furthermore, seven candidate proteins that potentially regulated XB130 expression by binding to the 113-230, 503-660, and 970-1,053 regions of the 3'-UTR were identified, shedding light on the regulatory mechanism of XB130 expression. Collectively, these results suggested that complex sequence integrations in the mRNA 3'-UTR variably affected XB130 expression in NSCLC cells.

Correspondence to: Professor Kewei Song or Professor Ying Liu, Key Laboratory of Endemic and Ethnic Diseases, Ministry of Education, Guizhou Medical University, 9 Beijing Road, Guiyang, Guizhou 550004, P.R. China
E-mail: fzsw-science@gmc.edu.cn
E-mail: 315324940@qq.com

*Contributed equally

Key words: non-small cell lung cancer, XB130, 3'-untranslated region, AU-rich element, mRNA stability

Introduction

XB130, an adaptor protein, plays essential roles in various biological processes, including cell proliferation, skeletal remodeling, endocytosis, migration, invasion, and epithelial-mesenchymal transformation (EMT) (1). XB130 can be phosphorylated by specific protein tyrosine kinases and subsequently interact with the P85α subunit of PI3K, thereby activating the PI3K/Akt signaling pathway (2,3). Dysregulation of XB130 has been observed in human gastrointestinal cancer, thyroid cancer, hepatocellular carcinoma, skin basal cell carcinoma, and other types of cancer, where it acts as either an oncogene or a tumor suppressor (1,4). Given its significance in cancer, further understanding of XB130 expression regulation is crucial for cancer clinical diagnosis, risk prediction, prognosis, and targeted therapy (1,5).

Previous studies have shown that silencing XB130 inhibits cell proliferation, migration, invasion, and EMT in non-small cell lung cancer (NSCLC) (6,7). Upregulated XB130 mRNA expression levels have been associated with improved survival in patients with NSCLC (1). Similarly, XB130 is poorly expressed in human gastric cancer and thyroid cancer, but *in vitro* experiments have shown that XB130 acts as an oncogene in these cancer types (1,8-10). To explain these contradictory findings, it has been suggested that XB130 is highly expressed in normal tissues, playing a vital role in maintaining normal cellular physiological activity. However, in cancer cells, the XB130-mediated signaling pathway may be manipulated to control cell proliferation, survival, and migration upon XB130 expression inhibition (1). Thus, investigating the regulatory mechanism of XB130 expression may provide insights into these paradoxical observations.

Post-transcriptional regulation is a critical form of eukaryotic gene expression modulation (11). The 3'-untranslated

region (3'-UTR) of mRNA contains numerous cis-acting elements involved in post-transcriptional regulation, such as microRNA (miRNA) binding sites and GU/AU/CU/U-rich elements (G/A/C/UREs), which regulate mRNA stability, subcellular localization and translation (11-14). G/A/C/UREs typically interact with specific RNA binding proteins (RBPs) to modulate gene expression (14-17). G/A/C/UREs have been found to be closely associated with tumor occurrence and inhibition (12-14). For example, the binding of heterogeneous nuclear ribonucleoprotein F (hnRNP F) to the AREs in the 3'-UTR of snail family transcriptional repressor 1 (SNAI1) mRNA promotes EMT in bladder cancer cells by stabilizing SNAI1 mRNA (18). In light of a previous report and sequence analysis, it was predicted that the XB130 3'-UTR contains three consensus AREs (sequence: AUUUA; ARE^{I}, ARE^{II}, and ARE^{III}), a specific URE (U_{19}), and several possible G/A/C/UREs (Fig. 1) (19). These elements may play critical roles in regulating XB130 mRNA stability and translation (19). Therefore, in the present study, the post-transcriptional regulation of XB130 expression was explored from this perspective.

In the present study, the entire XB130 3'-UTR (1,218 bp), as well as truncated fragments and mutant fragments with predicted ARE or URE deletions were cloned into the modified psiCHECK-2 vector. These recombinant constructs were then transfected into the PC-9 NSCLC cell line. Luciferase activity assays and reverse transcription-quantitative PCR (RT-qPCR) were performed to evaluate the impact of these insertions on reporter gene expression. Furthermore, candidate proteins that may regulate XB130 expression by binding to XB130 3'-UTR were screened for using RNA pull-down assays, followed by mass spectrometry and western blotting. This study may provide insights for further exploration of the regulatory mechanisms underlying XB130 expression.

Materials and methods

Cell culture and transfection. PC-9 and A549 NSCLC cell lines were used in the present study. PC-9 cells were purchased from FuHeng Biology Company, and A549 cells were obtained from the Type Culture Collection of the Chinese Academy of Sciences. Cells were maintained in RPMI 1640 medium (Gibco; Thermo Fisher Scientific, Inc.) supplemented with 10% FBS (Gibco; Thermo Fisher Scientific, Inc.) at 37˚C in a 5% CO_2 humidified atmosphere. Transfection of plasmids and small interfering RNAs (siRNAs) into NSCLC cells was performed using Entranster™-D4000 and Entranster™-R4000 (Engreen Biosystem), respectively, following the manufacturer's instructions. Unless otherwise noted, cells were collected for analysis 48 h after transfection. The sequences of the siRNAs used (Shanghai GenePharma, Co., Ltd.) are provided in Table I.

Plasmid construction. The dual-luciferase reporter vector psiCHECK-2 (Promega Corporation) was modified for the present study. Briefly, a chimeric intron was amplified from the psiCHECK-2 vector using specific primers (intron For and intron Rev) containing MluI and ApaI recognition sequences, respectively. The chimeric intron was then inserted into the 5'-UTR of the firefly luciferase gene ($hluc^{+}$) using MluI and ApaI cleavage sites. Various regions of the XB130 3'-UTR (1,218 bp, NM_032550.4) were amplified from the genomic DNA of PC-9 cells using the primers listed in Table II. The PCR thermocycling conditions were as follows: 35 amplification cycles of denaturation at 98˚C for 10 sec, annealing at 60˚C for 15 sec and extension at 72˚C for 60 sec, followed by final extension at 72˚C for 5 min. Mutant fragments with the deleted seed sequence, ATTTA, or T_{19} were obtained through overlap extension PCR (20). The PCR products were subsequently cloned into the 3'-UTR of the Renilla luciferase gene (hRluc) of the modified psiCHECK-2 vector. All plasmid constructs were confirmed by DNA sequencing.

Table I. Sequences of the small interfering RNAs.

Target gene	Direction	Sequence
ANXA2	Sense	GGAUGCUUUGAACAUUGAATT
	Antisense	UUCAAUGUUCAAAGCAUCCTT
FLNA	Sense	AGAAGAAGAUGCACCGCAATT
	Antisense	UUGCGGUGCAUCUUCUUCUTT
LMNA	Sense	CUGGACUUCCAGAAGAACATT
	Antisense	UGUUCUUCUGGAAGUCCAGTT
PLEC	Sense	CGGAGAUGGAGAAGCAUAATT
	Antisense	UUAUGCUUCUCCAUCUCCGTT
SPTAN1	Sense	CCUCAUGUCUUGGAUCAAUTT
	Antisense	AUUGAUCCAAGACAUGAGGTT
TPM1	Sense	CACGCUCUCAACGAUAUGATT
	Antisense	UCAUAUCGUUGAGAGCGUGTT
PKM	Sense	GAACUUCUCUCAUGGAACUTT
	Antisense	AGUUCCAUGAGAGAAGUUCTT
YBX3	Sense	GCAGGUGACCUAAAGAAUUTT
	Antisense	AAUUCUUUAGGUCACCUGCTT
MYH9	Sense	GGACCUUCCACAUCUUCUATT
	Antisense	UAGAAGAUGUGGAAGGUCCTT
CALU	Sense	CAGCCAUGAUGGGAAUACUTT
	Antisense	AGUAUUCCCAUCAUGGCUGTT
NC	Sense	UUCUCCGAACGUGUCACGUTT
	Antisense	ACGUGACACGUUCGGAGAATT

Dual-luciferase reporter assay. PC-9 cells were seeded into 48-well plates and transfected with the recombinant psiCHECK-2 constructs. After 48 h of transfection, Renilla and firefly luciferase activities were measured using a Luc-Pair™ Duo-Luciferase HS Assay Kit (GeneCopoeia, Inc.) according to the manufacturer's instructions. Briefly, cells were washed twice with PBS and lysed with 65 μl 1xLuc-Lysis II Buffer for 10 min at room temperature on a rotating wheel device. The luciferase assays were performed by sequentially adding 100 μl firefly and Renilla luciferase assay reagents to 20 μl cell lysate. The light output was measured using a BioTek Synergy2 Multimode Microplate Reader (Biotek Instruments, Inc.) immediately after adding each luciferase assay reagent. The $hluc^{+}$ gene served as the internal control.

RT-qPCR. Total RNA was isolated from cells using TRIzol® reagent (Invitrogen; Thermo Fisher Scientific, Inc.) according

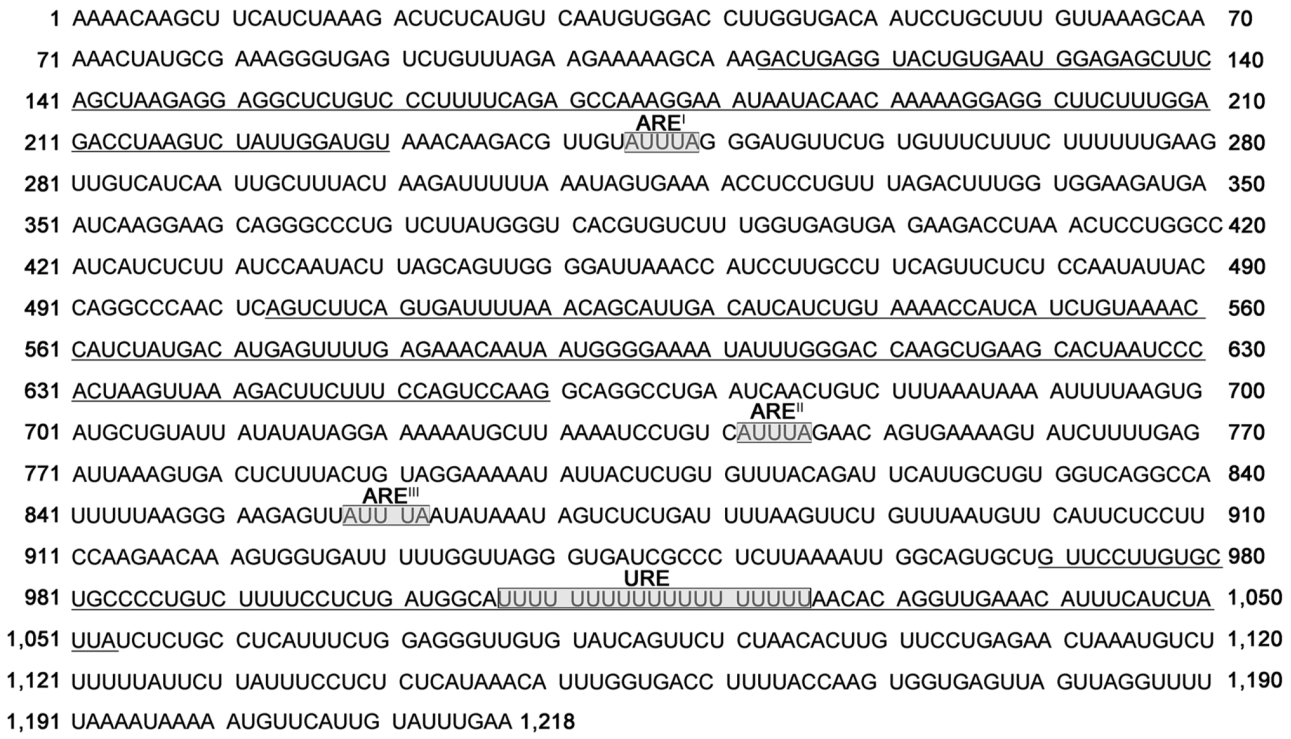

1 AAAACAAGCU UCAUCUAAAG ACUCUCAUGU CAAUGUGGAC CUUGGUGACA AUCCUGCUUU GUUAAAGCAA 70
71 AAACUAUGCG AAAGGGUGAG UCUGUUUAGA AGAAAAAGCA AAGACUGAGG UACUGUGAAU GGAGAGCUUC 140
141 AGCUAAGAGG AGGCUCUGUC CCUUUUCAGA GCCAAAGGAA AUAAUACAAC AAAAAGGAGG CUUCUUUGGA 210
211 GACCUAAGUC UAUUGGAUGU AAACAAGACG UUGUAUUUAG GGAUGUUCUG UGUUUCUUUC UUUUUUGAAG 280
281 UUGUCAUCAA UUGCUUUACU AAGAUUUUUA AAUAGUGAAA ACCUCCUGUU UAGACUUUGG UGGAAGAUGA 350
351 AUCAAGGAAG CAGGGCCCUG UCUUAUGGGU CACGUGUCUU UGGUGAGUGA GAAGACCUAA ACUCCUGGCC 420
421 AUCAUCUCUU AUCCAAUACU UAGCAGUUGG GGAUUAAACC AUCCUUGCCU UCAGUUCUCU CCAAUAUUAC 490
491 CAGGCCCAAC UCAGUCUUCA GUGAUUUUAA ACAGCAUUGA CAUCAUCUGU AAAACCAUCA UCUGUAAAAC 560
561 CAUCUAUGAC AUGAGUUUUG AGAAACAAUA AUGGGGAAAA UAUUUGGGAC CAAGCUGAAG CACUAAUCCC 630
631 ACUAAGUUAA AGACUUCUUU CCAGUCCAAG GCAGGCCUGA AUCAACUGUC UUUAAAUAAA AUUUUAAGUG 700
701 AUGCUGUAUU AUAUAUAGGA AAAAAUGCUU AAAAUCCUGU CAUUUAGAAC AGUGAAAAGU AUCUUUUGAG 770
771 AUUAAAGUGA CUCUUUACUG UAGGAAAAAU AUUACUCUGU GUUUACAGAU UCAUUGCUGU GGUCAGGCCA 840
841 UUUUUAAGGG AAGAGUUAUU UAAUAUAAAU AGUCUCUGAU UUUAAGUUCU GUUUAAUGUU CAUUCUCCUU 910
911 CCAAGAACAA AGUGGUGAUU UUUGGUUAGG GUGAUCGCCC UCUUAAAAUU GGCAGUGCUG UUCCUUGUGC 980
981 UGCCCCUGUC UUUUCCUCUG AUGGCAUUUU UUUUUUUUUU UUUUUAACAC AGGUUGAAAC AUUUCAUCUA 1,050
1,051 UUAUCUCUGC CUCAUUUCUG GAGGGUUGUG UAUCAGUUCU CUAACACUUG UUCCUGAGAA CUAAAUGUCU 1,120
1,121 UUUUUAUUCU UAUUUCCUCU CUCAUAAACA UUUGGUGACC UUUUACCAAG UGGUGAGUUA GUUAGGUUUU 1,190
1,191 UAAAAUAAAA AUGUUCAUUG UAUUUGAA 1,218

Figure 1. The sequence of XB130 3'-UTR. The cloned XB130 3'-UTR is 1,218 bp in length. The boxes show the three consensus AREs (ARE^{I}, ARE^{II}, and ARE^{III}) and a potential URE (U_{19}). Underlined sequences indicate the 113-230, 503-660, and 970-1,053 regions of the XB130 3'-UTR. UTR, untranslated region; ARE, AU-rich element; URE, U-rich element.

to the manufacturer's protocol. Reverse transcription was performed using a HyperScript III 1st Strand cDNA Synthesis Kit with gDNA Remover (NovaBio). The synthesized cDNA was quantified by qPCR using a 2x SYBR Green qPCR MasterMix (Bimake) on an Applied Biosystems StepOnePlus Real-Time PCR System (Applied Biosystems; Thermo Fisher Scientific, Inc.). The primer pairs qRL For and qRL Rev, and qFL For and qFL Rev (Table II) were used to amplify hRluc and $hluc^{+}$ cDNA, respectively. The quantity of hRluc mRNA in each sample was normalized to the $hluc^{+}$ content. For the expression of endogenous genes, GAPDH was used as the internal reference. The relative quantification of gene mRNA was calculated using the $2^{-\Delta\Delta Cq}$ method (21).

Reporter gene mRNA decay. To investigate the mRNA decay of a reporter gene, PC-9 cells were transiently transfected with the recombinant psiCHECK-2 constructs and incubated for 48 h. The transcription process was inhibited by adding 10 mg/ml actinomycin D. Cells were harvested at 0, 2, 4, and 6 h post-treatment, and total RNA was isolated. The hRluc and $hluc^{+}$ mRNA contents were determined by RT-qPCR. The relative hRluc mRNA levels, normalized to the $hluc^{+}$ mRNA content, are expressed as a percentage of the mRNA level at 0 h. Additionally, the levels of the endogenous gene heat shock protein 90 α family class A member 1 (Hsp90) and GAPDH mRNA were detected by RT-qPCR. GAPDH was used as the internal reference. The decay of Hsp90 mRNA was calculated using the aforementioned method.

RNA pull-down assay. Nucleotides 113-230, 503-660, or 970-1,053 of the XB130 3'-UTR were transcribed *in vitro* using a T7 RNA polymerase kit (Roche Diagnostics GmbH) and then labeled with Biotin using a Pierce RNA 3'End Desthiobiotinylation Kit according to the manufacturer's protocol (Invitrogen; Thermo Fisher Scientific, Inc.). The purified biotinylated RNA was incubated with streptavidin magnetic beads at room temperature for 15-30 min, followed by incubation with lysates from PC-9 cells at 4˚C for 30-60 min. The pulled-down proteins were subjected to mass spectrometry analysis by Sangon Biotech, Co., Ltd.

In silico co-expression analysis. The *in silico* co-expression analyses between RBPs and XB130 were performed using the ENCORI (https://rnasysu.com/encori/panGeneCoExp.php) and GEPIA2 (http://gepia2.cancer-pku.cn/#correlation) databases.

Western blotting. Harvested cells were lysed in RIPA Buffer (cat. no. P0013B; Beyotime Institute of Biotechnology) containing 1 mM PMSF (Beyotime Institute of Biotechnology) on ice for 30 min. After centrifugation at 14,000 x g for 15 min at 4˚C, the supernatants were collected. Protein samples were loaded on 12% SDS gels, resolved using SDS-PAGE, and transferred to PVDF membranes (cat. no. IPVH00010, MilliporeSigma). Following blocking with 5% BSA for 1 h, the membranes were incubated overnight at 4˚C with anti-XB130 (1:2,000, cat. no. 17183-1-AP; ProteinTech Group, Inc.) or anti-GAPDH (1:5,000, cat. no. 10494-1-AP; ProteinTech Group, Inc.) antibodies. Subsequently, the membranes were treated with a horseradish peroxidase-conjugated secondary antibody (1:5,000, cat. no. SA00001-2; ProteinTech Group, Inc.) for 1 h at 37˚C. The specific protein bands were visualized using an Enhanced Chemiluminescence Reagent

Table II. Sequences of primers.

Name	Sequence
Intron For	GTGACGCGTGTGGCCTCGAACACCGAGCGACCCTGCAGCGACCCGCTTAAAAGCTTGGCATTC CGGTAAGGTAAGTATCAAGGTTACAAGACAGG
Intron Rev	GCAGGGCCCTT CTTAATG TTCTTAGCATCGGCCATGGTGGCTTTACCAACCTGTGGAGAGAAA GGCAAAG
3'-UTR-1 For	CCGCTCGAGAAAACAAGCTTCATCTAAAG
3'-UTR-1,218 Rev	CGGGATCCTTCAAATACAATGAACATTT
3'-UTR-132 Rev	CGGGATCCCCATTCACAGTACCTCAGTC
3'-UTR-113 For	CCGCTCGAGGACTGAGGTACTGTGAATGG
3'-UTR-660 Rev	CGGGATCCCTTGGACTGGAAAGAAGTCT
3'-UTR-661 For	CCGCTCGAGGCAGGCCTGAATCAACTGTC
3'-UTR-795 Rev	CGGGATCCTCCTACAGTAAAGAGTCACT
3'-UTR-792 For	CCGCTCGAGAGGAAAAATATTACTCTGTG
3'-UTR-989 Rev	CGGGATCCACAGGGGCAGCACAAGGAAC
3'-UTR-970 For	CCGCTCGAGGTTCCTTGTGCTGCCCCTGT
ARE^{I} For	AACAAGACGTTGTGGGATGTTCTGTGTT
ARE^{I} Rev	CAGAACATCCCACAACGTCTTGTTTACAT
ARE^{II} For	TTAAAATCCTGTCGAACAGTGAAAAGTATC
ARE^{II} Rev	TTTCACTGTTCGACAGGATTTTAAGCA
ARE^{III} For	AAGGGAAGAGTTATATAAATAGTCTCTGA
ARE^{III} Rev	GACTATTTATATAACTCTTCCCTTAAAAATG
URE For	TCCTCTGATGGCAAACACAGGTTGAAAC
URE Rev	CAACCTGTGTTTGCCATCAGAGGAAAAGA
3'-UTR-230 Rev	CGGGATCCACATCCAATAGACTTAGGTC
3'-UTR-231 For	CCGCTCGAGAAACAAGACGTTGTATTTAG
3'-UTR-342 Rev	CGGGATCCCACCAAAGTCTAAACAGGAG
3'-UTR-343 For	CCGCTCGAGGAAGATGAATCAAGGAAGCA
3'-UTR-502 Rev	CGGGATCCGAGTTGGGCCTGGTAATATT
3'-UTR-503 For	CCGCTCGAGAGTCTTCAGTGATTTTAAAC
3'-UTR-1,053 Rev	CGGGATCCTAATAGATG AAATGTTTCAACCTGTGTTAA AAAAAAAAAAAAAAAAATGCC
3'-UTR-1,054 For	CCGCTCGAGTCTCTGCCTCATTTCTGGA
qRL For	TGGTCGTGAGGCACTGGGCAGGTG
qRL Rev	TGCTCGGGGTCGTACACCTTGGAA
qFL For	AAAGCTTGGCATTCCGGTAAGGTT
qFL Rev	GTGGGCATCGGTGAAGGCAA
qANXA2 For	TGCCTTCGCCTACCAGAGAA
qANXA2 Rev	GCCCAAAATCACCGTCTCC
qFLNA For	GGAGGAGGCAAAAGTGACCG
qFLNA Rev	ACTTATCCACGTACACCTCGAAG
qLMNA For	AATGATCGCTTGGCGGTCTAC
qLMNA Rev	CACCTCTTCAGACTCGGTGAT
qPLEC For	TGTACCGGCAGACCAACCT
qPLEC Rev	GCATGGCGTCATACAGCGA
qSPTAN1 For	GCCAACTCAGGAGCCATTGTT
qSPTAN1 Rev	CGGGTCCGTATGGTTTCAGAT
qTPM1 For	TTGAGAGTCGAGCCCAAAAAG
qTPM1 Rev	CATATTTGCGGTCGGCATCTT
qPKM For	ATGTCGAAGCCCCATAGTGAA
qPKM Rev	TGGGTGGTGAATCAATGTCCA
qYBX3 For	ACCGGCGTCCCTACAATTAC
qYBX3 Rev	GGTTCTCAGTTGGTGCTTCAC
qMYH9 For	CCTCAAGGAGCGTTACTACTCA
qMYH9 Rev	CTGTAGGCGGTGTCTGTGAT

Table II. Continued.

Name	Sequence
qCALU For	ATGGACCTGCGACAGTTTCTT
qCALU Rev	ACTCTGAGCATCATTGTGAACC
qGAPDH For	GGAGCGAGATCCCTCCAAAAT
qGAPDH Rev	GGCTGTTGTCATACTTCTCATGG

(cat. no. WBKLS0100; MilliporeSigma) and analyzed using a GeneGnome XRQ Chemiluminescence Imaging System (Syngene Europe).

Statistical analysis. Data are presented as the mean ± standard deviation (SD) of three independent experiments. Statistical analysis was performed using SPSS version 20 (IBM Corp.). Differences between two groups were determined using a Student's t-test. For comparisons involving ≥3, a one-way ANOVA followed by a post hoc Tukey's test was used. In the case of mRNA decay analysis, a repeated-measures ANOVA followed by a post hoc Dunnett's test was used. $P<0.05$ was considered to indicate a statistically significant difference.

Results

XB130 3'-UTR insertion promotes the expression of a reporter gene. To investigate the effect of the XB130 3'-UTR on gene expression, various regions of the XB130 3'-UTR were inserted into the 3'-UTR of the hRluc reporter gene in the dual-luciferase reporter vector, psiCHECK-2. hRluc was used as the reporter, while hluc$^+$ served as the internal control. In all reporter constructs, hRluc was controlled by identical promoter elements and followed by different XB130 3'-UTR fragments, thus any changes observed in luciferase activity would be attributed to alterations in either mRNA stability or translation rate. Additionally, to avoid plasmid DNA contamination during mRNA sample measurement, the psiCHECK-2 vector was modified as described by Tao and Gao (22). To detect the levels of hRluc and hluc$^+$ mRNA transcribed from the recombinant plasmids, two forward primers (qRL For and qFL For) that spanned the chimeric intron, along with their respective reverse primers, were designed (Fig. 2A).

The recombinant constructs shown in Fig. 2B were transfected into PC-9 cells, and the luciferase activities were analyzed 48 h after transfection. As shown in Fig. 2C, inserting the entire XB130 3'-UTR (nucleotides 1-1,218) into the hRluc 3'-UTR significantly increased luciferase activity by 3.57-fold compared with the control group (Ctrl). Deletion of nucleotides 990-1,218 from the entire 3'-UTR led to an increase in luciferase activity by 1.34-fold compared with the 1-1,218 3'-UTR group. Truncation of the 3'-UTR from nucleotide 796 or 661 to 1,218 did not have an additional effect on luciferase activity compared with the 1-989 3'-UTR group. However, further truncation from nucleotide 660 to 133 resulted in a significant 0.77-fold decrease in luciferase activity compared with the 1-660 3'-UTR group. Notably, the 1-132 3'-UTR group still exhibited high luciferase activity at 3.59-fold higher than the Ctrl group. These findings suggested the presence of positive regulatory elements in nucleotides 1-660 and negative regulatory elements in nucleotides 990-1,218 of the XB130 3'-UTR.

Deleting the 5' regions of the XB130 3'-UTR revealed different results. As shown in Fig. 2D, the deletion of the first 112 nucleotides increased luciferase activity by 1.25-fold compared with the 1-1,218 3'-UTR group, indicating the presence of negative regulatory elements in nucleotides 1-112. Gradually truncation from the proximal region to nucleotides 660, 791, and 969 resulted in a decrease in luciferase activity, suggesting the presence of positive regulatory elements in nucleotides 113-969. Notably, insertion of the 970-1,218 3'-UTR into psiCHECK-2 had no significant effect on luciferase activity compared with the Ctrl group. Overall, these results indicated the presence of negative regulatory elements in nucleotides 1-112 and 990-1,218, and positive regulatory elements in nucleotides 113-989. Additionally, the effect of the 660-989 3'-UTR fragment on luciferase activity appeared to be context-dependent.

A URE in the XB130 3'-UTR inhibits the expression of a reporter gene. A previous study reported the presence of two consensus AREs (ARE^{II}, nucleotides 742-746 and ARE^{III}, nucleotides 858-862) in the XB130 3'-UTR (Fig. 1), which may play a role in regulating mRNA stability and translation rate (19). Another consensus ARE (ARE^{I}, nucleotides 245-249) and a potential URE (nucleotides 1,007-1,025) were also identified (Fig. 1). To determine the effects of these elements on gene expression, recombinant psiCHECK-2 plasmids containing XB130 3'-UTR fragment 113-660, 661-795, 792-989, or 970-1,218, as well as the corresponding mutant plasmids with ARE or URE deletions (113-660-ARE^{I}, 661-795-ARE^{II}, 792-989-ARE^{III}, or 970-1,218-URE), were constructed (Fig. 3A). As shown in Fig. 3B, the insertion of the 113-660, 661-795, or 792-989 3'-UTR fragments significantly increased luciferase activity by 4.10-fold, 2.06-fold, and 1.68-fold, respectively, compared with the Ctrl group. These findings further supported the presence of positive regulatory elements in the 113-989 region of the 3'-UTR. Notably, deletion of ARE^{I}, ARE^{II}, or ARE^{III} did not have a significant effect on luciferase activity compared with the corresponding wild-type constructs (Fig. 3B). However, deletion of the URE resulted in 1.81-fold higher expression of the reporter gene compared with the 970-1,218 3'-UTR group, suggesting that the URE had a negative effect on gene expression.

Regions 113-230, 503-660, and 970-1,053 of the XB130 3'-UTR significantly affect the expression of a reporter gene. Based on the aforementioned results, the 113-660 region and

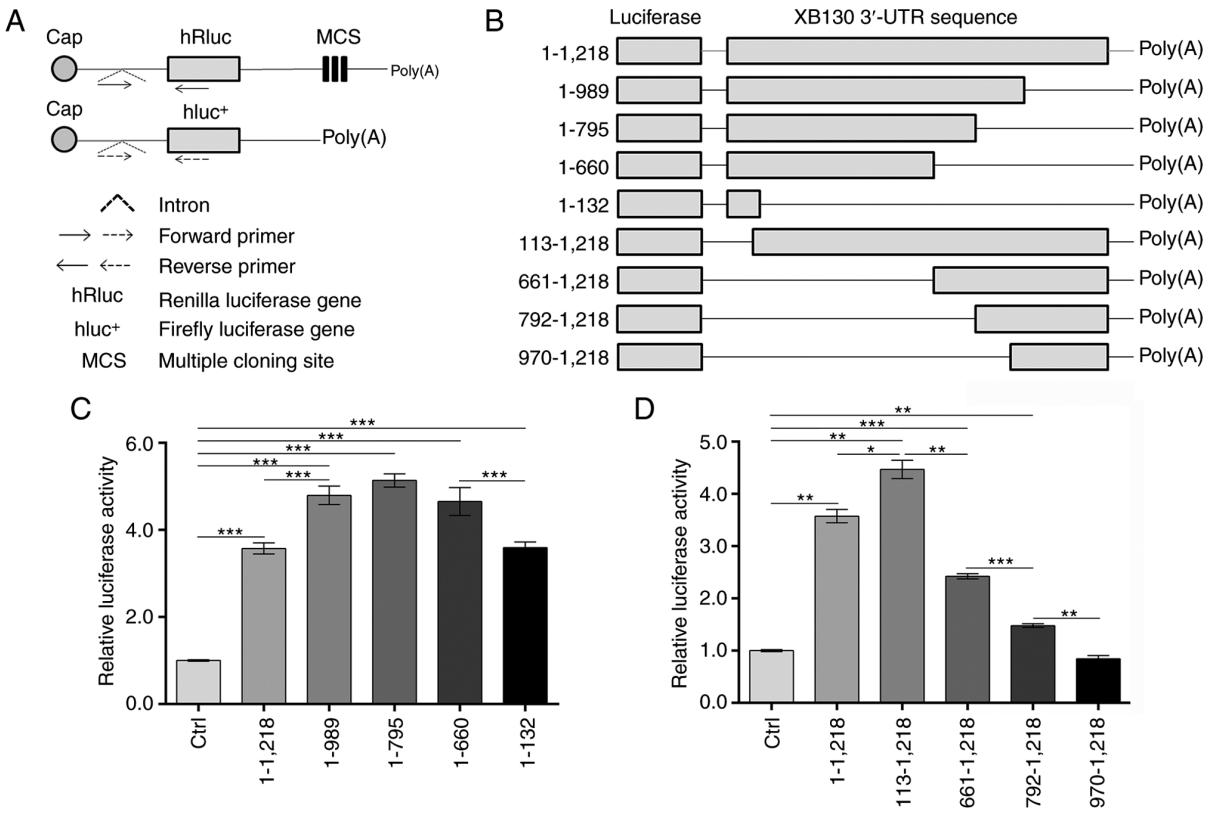

Figure 2. XB130 3'-UTR insertion enhances luciferase activity. (A) Schematic of the psiCHECK-2 vector modification and RT-qPCR primer design. (B) Construction of recombinant plasmids via insertion of the different regions of the XB130 3'-UTR into the modified psiCHECK-2 vectors. Numbering starts from the nucleotide following the stop codon for XB130. (C and D) PC-9 cells were transfected with the empty modified psiCHECK-2 vector or the recombinants. After 48 h, Renilla and firefly luciferase activity was measured. The ratio of Renilla/firefly luciferase activity was calculated, and the relative luciferase activity is expressed as a multiple of that measured in the Ctrl group. *P<0.05, **P<0.01, ***P<0.001. UTR, untranslated region; RT-qPCR, reverse transcription-quantitative PCR; hRluc, Renilla luciferase gene; MCS, multiple cloning site; hluc^{+}, firefly luciferase gene; Ctrl, control.

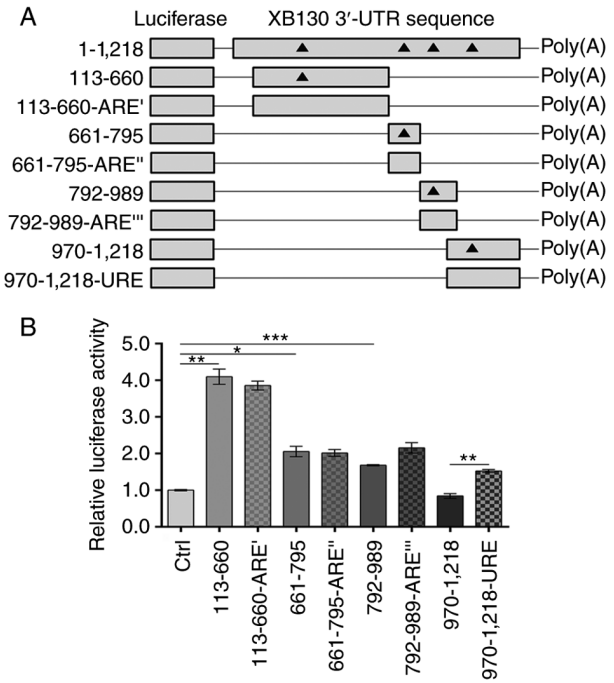

Figure 3. A URE in XB130 3'-UTR inhibits luciferase activity. (A) Overview of the construction of the recombinant constructs. '▲' indicates the predicted ARE^{I}, ARE^{II}, ARE^{III}, or URE. (B) PC-9 cells were transfected with the empty modified psiCHECK-2 vector or the recombinants. The luciferase activity was measured after 48 h. *P<0.05, **P<0.01, ***P<0.001. UTR, untranslated region; ARE, AU-rich element; URE, U-rich element; Ctrl, control.

the URE in the XB130 3'-UTR were identified as having the most pronounced positive and negative effects on the expression of the reporter gene, respectively. To facilitate subsequent screening of the combined RBPs, the 113-660 3'-UTR fragment was further divided into smaller fragments: 113-230, 231-342, 343-502, and 503-660. Additionally, the 970-1,218 3'-UTR fragment was truncated into 970-1,053 and 1,054-1,218 fragments, of which the identified URE was located in the 970-1,053 3'-UTR fragment. The corresponding recombinant psiCHECK-2 plasmids were constructed (Fig. 4A) and transfected into PC-9 cells, to measure the luciferase activity and steady-state mRNA levels. The results demonstrated that the insertion of the 113-230 or 503-660 3'-UTR fragment significantly increased the luciferase activity (Fig. 4B) and steady-state mRNA levels (Fig. 4C), compared with the Ctrl group, indicating that the 113-230 and 503-660 regions of the 3'-UTR promoted reporter gene expression, possibly through increased mRNA stability. However, the insertion of the 970-1,053 3'-UTR fragment resulted in a significant decrease in luciferase activity (Fig. 4B), but an increase in the steady-state mRNA levels of the luciferase gene (Fig. 4C), compared with the Ctrl group. This suggested that the 970-1,053 region of the 3'-UTR may hinder reporter gene expression by reducing the translation rate of the luciferase mRNA.

XB130 3'-UTR 113-230, 503-660, or 970-1,053 fragment insertion increases the mRNA stability of a reporter gene. To

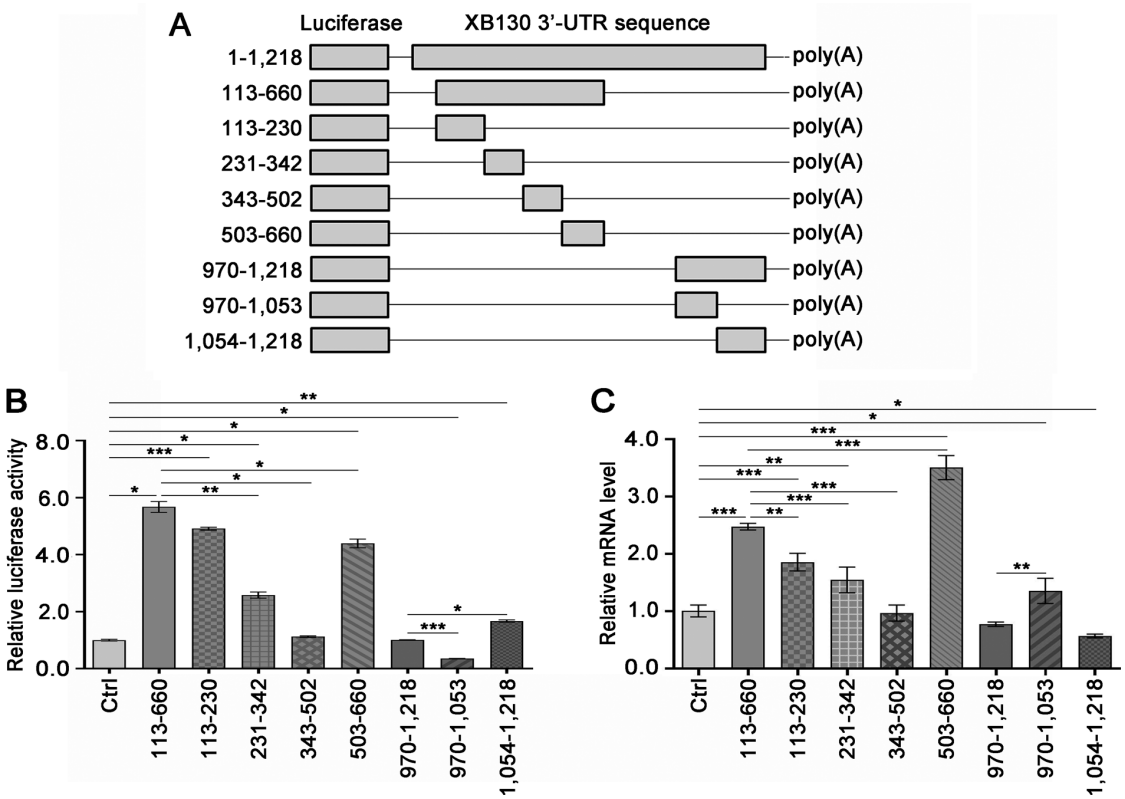

Figure 4. Regions 113-230, 503-660, and 970-1,053 of the XB130 3'-UTR significantly affect the luciferase activity and mRNA levels. (A) Overview of the construction of the recombinant constructs. (B and C) PC-9 cells were transfected with the empty modified psiCHECK-2 vector or the recombinants. The luciferase activity and mRNA levels were measured after 48 h. The hRluc mRNA levels were normalized to the hluc$^+$ mRNA level, and the relative mRNA level was expressed as a multiple of that measured in the Ctrl group. *P<0.05, **P<0.01, ***P<0.001. UTR, untranslated region; Ctrl, control; hluc$^+$, firefly luciferase gene; Ctrl, control.

understand the molecular mechanism underlying the regulation of reporter gene expression by the aforementioned fragments, their effects on mRNA stability were investigated. As shown in Fig. 5, all the tested fragments increased the mRNA stability of the reporter gene, which was consistent with the observed steady-state mRNA levels of the reporter gene in Fig. 4C. Furthermore, compared to the Ctrl group, no alteration was observed in the stability of Hsp90 mRNA within the 113-230, 503-660, or 970-1,053 3'-UTR groups (Fig. 5). These findings suggested that the 113-230 and 503-660 regions of the 3'-UTR promoted the expression of the reporter gene by enhancing mRNA stability.

XB130 3'-UTR 113-230, 503-660, or 970-1,053 fragment insertion impairs mRNA translation of a reporter gene. To assess the relative contribution of mRNA translation rate to the expression of the reporter gene, the relative enzymatic activity level (Fig. 4B) to the relative mRNA level (Fig. 4C) of luciferase was calculated for each group. A ratio of 1 indicated a direct correlation between protein and mRNA levels, suggesting no contribution of the translation process to reporter gene expression. Ratios >1 indicated a positive contribution of the translation process to reporter gene expression, while ratios <1 indicated a negative contribution. The larger the deviation from 1, the greater the positive or negative impact of translation.

The results listed in Table III indicated that the 113-230 3'-UTR fragment had a relatively high ratio, the 503-660 fragment had a ratio slightly >1 and the 970-1,053 fragment had a ratio significantly <1. These results suggested that the 113-230 and 503-660 regions of the 3'-UTR promoted reporter gene expression through a combination of positive contributions from mRNA stability and translation rate. By contrast, the 970-1,053 region of the 3'-UTR inhibited reporter gene expression due to translation inhibition.

Seven RBPs potentially regulate XB130 expression by binding to the 113-230, 503-660, or 970-1,053 region of the XB130 3'-UTR. Typically, the mRNA 3'-UTR influences mRNA stability or translation rate by binding to specific RBPs. Given the significant influence of the 113-230, 503-660, or 970-1,053 XB130 3'-UTR fragment insertion on reporter gene expression, further screening for RBPs that bind to these regions may shed light on the regulatory mechanism of XB130 expression. RNA pull-down assays and mass spectrometry analysis were conducted, resulting in the identification of 29, 31, or 12 candidate RBPs that bound to the 113-230, 503-660, or 970-1,053 XB130 3'-UTR fragment, respectively (Tables IV, SI and SII). To validate the potential interactions between candidate RBPs and XB130, *in silico* co-expression analyses were performed using the ENCORI and GEPIA2 databases. Considering that the insertion of the 113-230, 503-660, or 970-1,053 XB130 3'-UTR fragment increased reporter gene mRNA stability, the mRNA expression levels of candidate RBPs were expected to be positively correlated with XB130

Table III. Comparison of the enzymatic activity and mRNA level of the luciferase.

Region of 3'-UTR	Enzymatic activity level	mRNA level	Ratio[a]
Control	1.00±0.03	1.00±0.10	1.00±0.03
113-660	5.68±0.19	2.48±0.06	2.29±0.08
113-230	4.91±0.05	1.86±0.15	2.64±0.03
231-342	2.58±0.11	1.55±0.22	1.67±0.07
343-502	1.12±0.03	0.97±0.14	1.16±0.03
503-660	4.40±0.15	3.51±0.21	1.25±0.04
970-1,218	1.01±0.00	0.77±0.04	1.30±0.01
970-1,053	0.35±0.01	1.35±0.22	0.26±0.01
1,054-1,218	1.67±0.04	0.57±0.03	2.94±0.07

[a]A ratio of 1 indicates a direct correlation between protein and mRNA levels. A ratio >1 indicates a positive contribution at the translation level. A ratio <1 indicates a negative contribution at the translation level. The magnitude of the deviation from 1 reflects the extent of the positive or negative contribution.

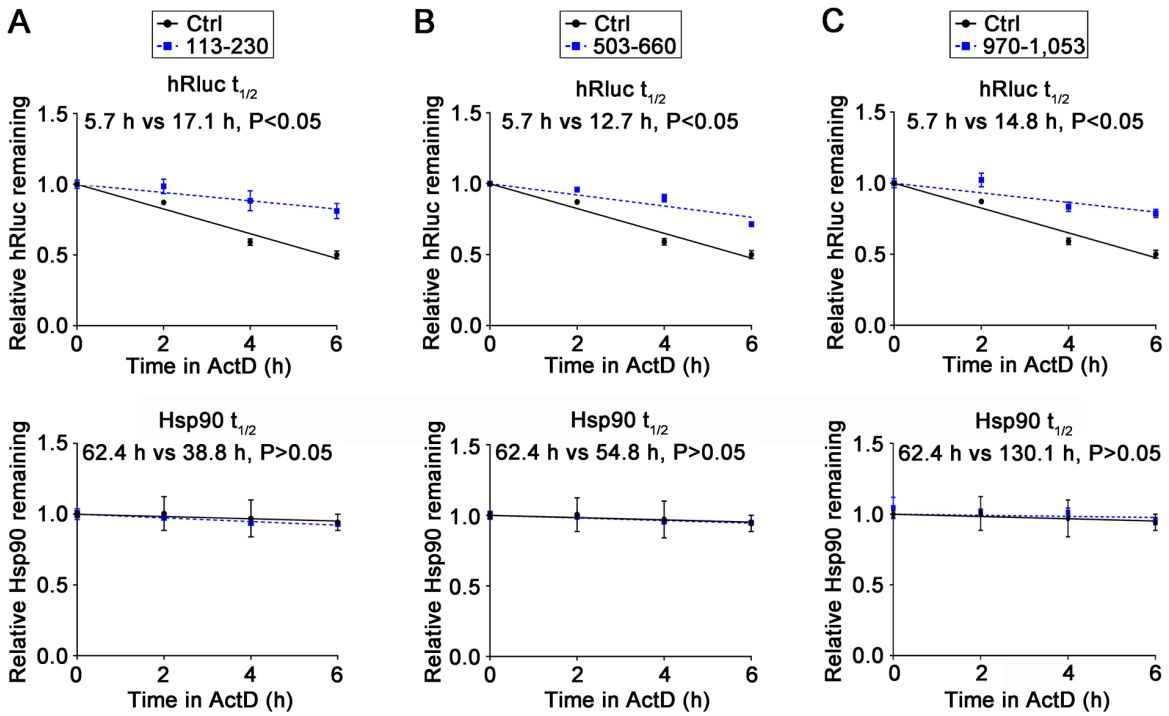

Figure 5. XB130 3'-UTR 113-230, 503-660, or 970-1,053 fragment insertion increases luciferase mRNA stability. PC-9 cells were transfected with the empty modified psiCHECK-2 vector or the recombinant containing the (A) 113-230 region, (B) 503-660 region or (C) 970-1,053 region of the XB130 3'-UTR. After 48 h, ActD (10 μg/ml) was added. At 0, 2, 4, and 6 h post-treatment, cells were collected for RNA extraction, and the mRNA expression levels of luciferase and Hsp90 were measured by RT-qPCR. The hRluc mRNA level was normalized to the hluc$^+$ mRNA levels, and Hsp90 mRNA levels were normalized to GAPDH mRNA levels. UTR, untranslated region; hluc$^+$, firefly luciferase gene; Ctrl, control; $t_{1/2}$, the half-lives of hRluc and Hsp90 mRNA; ActD, actinomycin D.

mRNA expression level. As shown in Fig. 6, 10 candidate RBPs were screened for co-expression with XB130 in both databases. Among them, Annexin A2 (ANXA2), Filamin-A (FLNA), Lamin A/C (LMNA), Plectin (PLEC), Spectrin α, non-erythrocytic 1 (SPTAN1), and Tropomyosin 1 (TPM1) were identified as candidate RBPs for the 113-230 region of the 3'-UTR, while ANXA2, FLNA, Pyruvate kinase M1/2 (PKM), and Y-box binding protein 3 (YBX3) were identified as candidate RBPs for the 503-660 region of the 3'-UTR. In addition, myosin heavy chain 9 (MYH9) and calumenin (CALU) were candidate RBPs for the 970-1,053 region of the 3'-UTR.

Following this analysis, the expression of each RBP candidate was knocked down in two NSCLC cell lines, and the XB130 mRNA and protein levels were measured. The results demonstrated that knockdown of ANXA2, FLNA, LMNA, SPTAN1, TPM1, YBX3, or CALU downregulated XB130 mRNA and protein expression in both NSCLC cell lines (Fig. 7). This indicated that these seven RBPs may regulate XB130 expression by binding to the 113-230, 503-660, or 970-1,053 region of the XB130 3'-UTR.

Table IV. Candidate RBPs that bind to the 113-230, 503-660, or 970-1,053 region of the XB130 3'-UTR identified by RNA pull-down and mass spectrometry analyses.

XB130 3'-UTR region	Gene	Protein name	mW, kDa
113-230	TUBB3	Tubulin β 3 class III	50.433
	ACTC1	Actin α cardiac muscle 1	42.019
	TUBA1C	Tubulin α1c	49.895
	TPM1	Tropomyosin 1	31.753
	HIST1H2BK	H2B clustered histone 12	13.89
	HIST1H2AB	H2A clustered histone 4	14.135
	HNRNPR	Heterogeneous nuclear ribonucleoprotein R	70.943
	LDHA	Lactate dehydrogenase A	36.689
	YWHAB	Tyrosine 3-monooxygenase/tryptophan 5-monooxygenase activation protein β	28.082
	LMNB2	Lamin-B2	69.948
	SYNCRIP	Heterogeneous nuclear ribonucleoprotein Q	69.603
	NDUFS3	NADH: ubiquinone oxidoreductase core subunit S3	30.242
	HSP90B1	Heat shock protein 90 β family member 1	92.469
	IMMT	Inner membrane mitochondrial protein	83.678
	PPL	Periplakin	204.747
	PHB	Prohibitin 1	29.804
	SPTAN1	Spectrin α, non-erythrocytic 1	284.539
	FLNA	Filamin-A	280.739
	RNH1	Ribonuclease/angiogenin inhibitor 1	49.973
	INA	Internexin neuronal intermediate filament protein α	55.391
	NCL	Nucleolin	76.614
	GAPDH	Glyceraldehyde-3-phosphate dehydrogenase	36.053
	ANXA2	Annexin A2	38.604
	RAE1	Ribonucleic acid export 1	40.968
	PLEC	Plectin	531.791
	LMNB1	Lamin-B1	66.408
	ATP5PD	ATP synthase peripheral stalk subunit d	18.491
	LMNA	Lamin A/C	74.139
	HSPA8	Heat shock protein family A (Hsp70) member 8	70.898
503-660	TUBB3	Tubulin β3 class III	50.433
	HIST1H2BK	H2B clustered histone 12	13.89
	HIST1H2AB	H2A clustered histone 4	14.135
	HNRNPR	Heterogeneous nuclear ribonucleoprotein R	70.943
	LDHA	Lactate dehydrogenase A	36.689
	HNRNPK	Heterogeneous nuclear ribonucleoprotein K	50.976
	H2AFZ	H2A.Z variant histone 1	13.553
	PKM	Pyruvate kinase M1/2	57.937
	YWHAB	Tyrosine 3-monooxygenase/tryptophan 5-monooxygenase activation protein β	28.082
	SYNCRIP	Heterogeneous nuclear ribonucleoprotein Q	69.603
	NDUFS3	NADH: ubiquinone oxidoreductase core subunit S3	30.242
	YBX3	Y-box binding protein 3	40.09
	YWHAE	Tyrosine 3-monooxygenase/tryptophan 5-monooxygenase activation protein ε	29.174
	HNRNPD	Heterogeneous nuclear ribonucleoprotein D	38.434
	IMMT	Inner membrane mitochondrial protein	83.678
	ALDOA	Aldolase, fructose-bisphosphate A	39.42
	HSP90B1	Heat shock protein 90 β family member 1	92.469
	RPL4	Ribosomal protein L4	47.697
	GAPDH	Glyceraldehyde-3-phosphate dehydrogenase	36.053
	EIF2AK2	Eukaryotic translation initiation factor 2 α kinase 2	62.094
	FLNA	Filamin-A	280.739

Table IV. Continued.

XB130 3'-UTR region	Gene	Protein name	mW, kDa
	RBMX	RNA binding motif protein X-linked	42.332
	RPS10	Ribosomal protein S10	18.898
	RPS14	Ribosomal protein S14	16.273
	HIST1H2BJ	H2B clustered histone 11	13.904
	ANXA2	Annexin A2	38.604
	RPL12	Ribosomal protein L12	17.819
	RPS19	Ribosomal protein S19	16.061
	LRRC59	Leucine rich repeat containing 59	34.93
	HSPD1	Heat shock protein family D (Hsp60) member 1	61.055
	HNRNPAB	Heterogeneous nuclear ribonucleoprotein A/B	30.303
970-1,053	HNRNPD	Heterogeneous nuclear ribonucleoprotein D	38.434
	H2AFZ	H2A.Z variant histone 1	13.553
	PTBP1	Polypyrimidine tract binding protein 1	57.221
	CD2BP2	CD2 cytoplasmic tail binding protein 2	37.646
	PFN1	Profilin-1	15.054
	HNRNPC	Heterogeneous nuclear ribonucleoproteins C	33.67
	ESRP1	Epithelial splicing regulatory protein 1	75.585
	HNRNPAB	Heterogeneous nuclear ribonucleoprotein A/B	30.303
	PGRMC1	Progesterone receptor membrane component 1	21.671
	MYH9	Myosin heavy chain 9	226.532
	HNRNPDL	Heterogeneous nuclear ribonucleoprotein D-like	46.438
	CALU	Calumenin	37.107

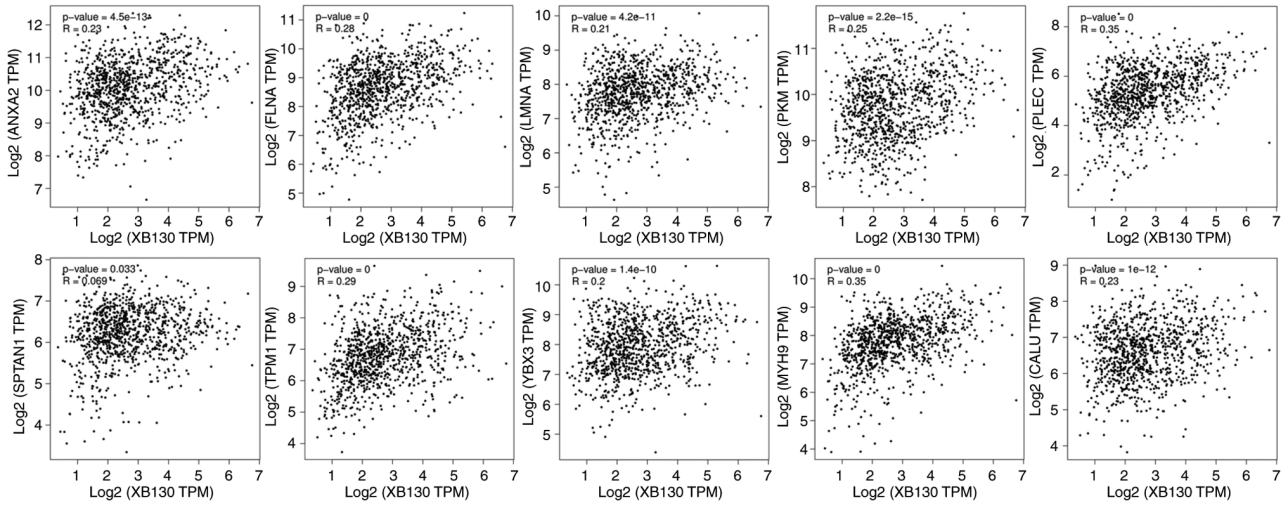

Figure 6. A total of 10 candidate RBPs that potentially bind to the 113-230, 503-660, or 970-1,053 region of the XB130 3'-UTR were identified through bioinformatics analysis. *In silico* co-expression analysis between each RBP candidate and XB130 was performed using the ENCORI and GEPIA2 databases. RBP, RNA binding protein; UTR, untranslated region; TPM, transcripts per million.

Discussion

To date, the function of XB130 protein has been well elucidated, but there has been limited research on the regulation of its expression (1-6,10,19,23-27). Previous studies have demonstrated that overexpression of miR-30a/b/c/d/e, 203, 219, or 4782-3p inhibited XB130 expression, impacting the proliferation, migration, invasion, and EMT of NSCLC cells (6,7). The present study demonstrated that, apart from miRNA binding sites, other positive and negative regulatory elements are present in the XB130 3'-UTR, of which negative regulatory elements were primarily located in the 1-112 and 990-1,218 regions of the 3'-UTR, and positive regulatory elements in the 113-989 region.

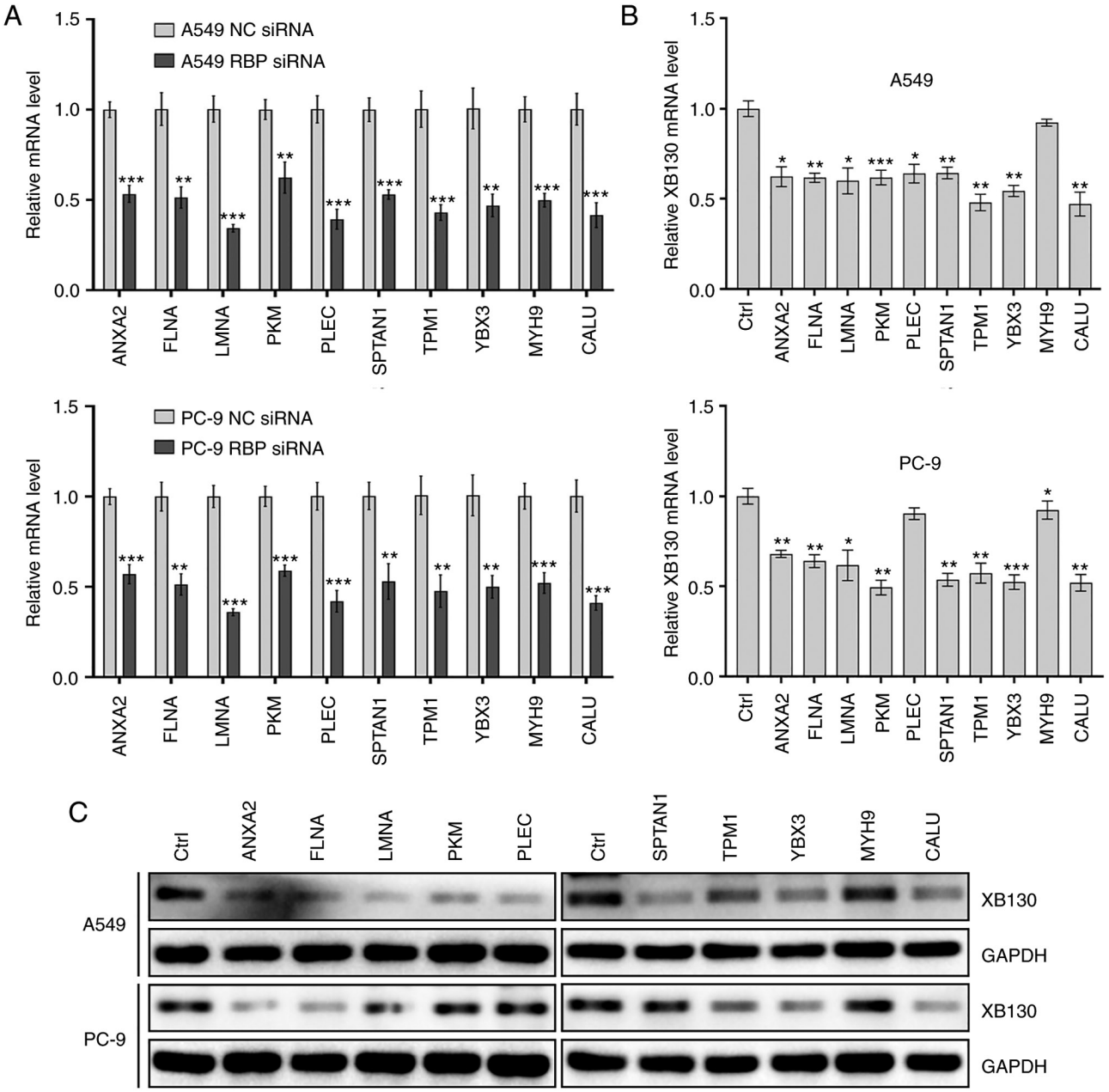

Figure 7. A total of seven RBPs were predicted to regulate XB130 mRNA and protein expression in A549 and PC-9 cells. A549 and PC-9 cells were transfected with siRNAs targeting RBPs or control (NC) siRNA, and the expression of each RBP and XB130 at the mRNA level as well as XB130 protein expression levels were measured after 48 h. (A) The knockdown efficiency of each RBP siRNA was determined by RT-qPCR. (B) XB130 mRNA levels were measured by RT-qPCR after transfection of each siRNA targeting an RBP. (C) XB130 protein levels were measured by western blotting after transfection of each siRNA targeting an RBP. GAPDH was used as the internal control. *P<0.05, **P<0.01, ***P<0.001 vs. NC siRNA or Ctrl group. RBP, RNA binding protein; NC, negative control; Ctrl, control; siRNA, small interfering RNA; RT-qPCR, reverse transcription-quantitative PCR.

The present study indicated that the insertion of the 661-795 or 792-989 3'-UTR fragments into the psiCHECK-2 vector increased the luciferase activity of the reporter gene, compared with the Ctrl group. Furthermore, compared with the 970-1,218 3'-UTR group, the addition of 792-969 or 661-969 3'-UTR fragment to the 5'-end of the 970-1,218 3'-UTR fragment further enhanced luciferase activity, suggesting the presence of positive regulatory elements in the 661-989 region of the 3'-UTR. However, compared with the 1-660 3'-UTR group, the insertion of the 661-795 or 661-989 3'-UTR fragments at the 3'-end of the 1-660 3'-UTR fragment did not further promote reporter gene expression. This observation indicated that the presence of the 1-660 region of the 3'-UTR inhibited the activity of positive regulatory elements in the 661-989 region of the 3'-UTR. Similarly, Cok and Morrison (28) reported that the 373-792 region of the Cyclooxygenase-2 (COX-2) 3'-UTR alone exerted an inhibitory effect on gene expression, but exhibited a positive regulatory property when combined with the 1-373 region of the COX-2 3'-UTR.

Based on the A/URE classification principles, XB130 3'-UTR contains three typical IIE AREs (ARE^{I}, ARE^{II}, and ARE^{III}) and one potential URE (15,29,30). In the present study, these elements were investigated through deletion mutations. The results demonstrated that the deletion of the three AREs did not affect luciferase

activity, while the deletion of the URE increased luciferase activity, indicating that the URE acts as a negative regulation element for XB130 expression. Additionally, the insertion of the 970-1,053 3'-UTR fragment, where the URE is located, increased luciferase mRNA stability but reduced luciferase activity. Based on these results, it is hypothesized that the predicted URE may possess functions that promote mRNA stability while inhibiting mRNA translation rate. Similar functions of G/A/C/UREs have been previously reported. For example, CUGBP Elav-like family member 2 (CUGBP2) increased the stability of COX-2 mRNA and inhibited mRNA translation by binding to two AREs in the COX-2 3'-UTR, resulting in decreased COX-2 expression (31). In addition, human antigen R (HuR) or AU-rich binding factor 1 (AUF1) reduced the expression of tumor necrosis factor-α or granulocyte-macrophage colony-stimulating factor, respectively, through a similar mechanism (32,33).

Among the G/A/C/UREs, AREs and GREs have been more extensively studied. AREs are present in 10-15% of human mRNAs and they regulate cell signaling, RNA metabolism, growth, and development by interacting with specific RBPs, such as Tristetraprolin, HuR, AUF1, and KH-type splicing regulatory protein (16,34,35). Comparatively, research on GRE is relatively scarce (16). GRE is found in at least 5% of human mRNA, its core sequence is GUUUG, and it is primarily involved in cell transcription, cell cycle, cell metabolism, and cell-cell communication (14,16). Several GRE-binding proteins have been identified, including CUGBP Elav-like family member 1, CUGBP2, and HuR (14,17). Regarding CRE, it has been reported that the core sequence is (C/U)CCAN$_x$CCC(U/A)(C/U)$_y$UC(C/U)CC, and hnRNP K or E2/E1 can stabilize mRNA by binding to the CRE (36,37). In the present study, it was observed that the insertion of the 113-230 or 503-660 XB130 3'-UTR fragment significantly increased luciferase activity. However, the core sequences of ARE, GRE, and CRE were not identified in the 113-230 and 503-660 regions of the 3'-UTR. Therefore, it is speculated that atypical G/A/C/URE sequences may exist in these regions, such as AGUUU, which requires further investigation through truncation or mutation experiments.

In the present study, seven candidate RBPs were identified that regulated XB130 mRNA and protein expression in two cell lines. Among them, LMNA is a major component of the mammalian nuclear lamina and is involved in regulating cellular signaling and gene transcription (38). CALU is a Ca^{2+}-binding protein located within the endoplasmic reticulum (39). SPTAN1 and TPM1 are cytoskeletal proteins associated with cell adhesion, DNA repair, and cell migration (40,41). Currently, their participation in post-transcriptional regulation of gene expression remains unclear. In the present study, knockdown of CALU, a candidate RBP of the 970-1,053 region of the XB130 3'-UTR, decreased XB130 mRNA and protein expression levels, suggesting that CALU primarily regulated XB130 mRNA stability. The 970-1,053 region of the 3'-UTR may suppress XB130 translation by binding to other unidentified RBPs. ANXA2 has been reported to post-transcriptionally regulate the expression of c-Myc and prolyl 4-hydroxylase subunit α 1 genes by binding to the AA(C/G)(A/U)G consensus sequence in their 3'-UTRs (42). Furthermore, Cheng and Tong (43) reported that FLNA and ANXA2 interacted and cooperatively mediated gefitinib resistance in NSCLC. Given the presence of the AA(C/G)AG sequence in the 113-230 and 503-660 regions of the XB130 3'-UTR, it is plausible that the interaction between FLNA and ANXA2 promotes ANXA2 binding to these regions of the 3'-UTR, subsequently enhancing XB130 mRNA stability or translation rate. YBX3 has been shown to bind to the 3'-UTR of solute carrier family 7 member 5 and stabilize its transcript for translation (44). Therefore, it is suggested that YBX3 may bind to the 503-660 region of the XB130 3'-UTR, thereby enhancing the stability of XB130 mRNA.

In conclusion, the present study highlighted the significant role of the XB130 3'-UTR as a crucial regulator of XB130 expression by modulating mRNA stability and translational rate. Specifically, the 113-230, 503-660, and 970-1,053 regions of the 3'-UTR may play a critical role by interacting with specific RBPs, including ANXA2, FLNA, LMNA, SPTAN1, TPM1, YBX3 and CALU. It is important to note that further research is needed to verify the binding between these RBPs and the mentioned 3'-UTR fragments, as well as their impact on XB130 mRNA stability and translation. Despite these limitations, the findings of the present study provide a strong basis for future investigations into the mechanisms governing XB130 expression.

Acknowledgements

Not applicable.

Funding

This work was supported by the National Natural Science Foundation of China (grant nos. 81660474 and 81960655), the Guizhou Provincial Basic Research Program (Natural Science) (grant nos. ZK[2022]041 and ZK[2022]372), the Academic Seedling Project of Guizhou Medical University (grant no. 21NSFCP04), and the Natural Science Foundation of Guizhou Provincial Health Commission (grant no. gzwkj2023-254).

Availability of data and materials

The datasets used and/or analyzed during the current study are available from the corresponding author upon reasonable request.

Authors' contributions

QW, YL, and KS designed the study. QW and LL performed the experiments, prepared the figures, and wrote the manuscript. XG and TZ performed the statistical analysis. YZ, YX, and JZ interpreted the data. QW, YL, and KS confirm the authenticity of all the raw data. All authors read and approved the final manuscript.

Ethics approval and consent to participate

Not applicable.

Patient consent for publication

Not applicable.

Competing interests

The authors declare that they have no competing interests.

References

1. Bai XH, Cho HR, Moodley S and Liu M: XB130-A novel adaptor protein: Gene, function, and roles in tumorigenesis. Scientifica (Cairo) 2014: 903014, 2014.
2. Lodyga M, De Falco V, Bai XH, Kapus A, Melillo RM, Santoro M and Liu M: XB130, a tissue-specific adaptor protein that couples the RET/PTC oncogenic kinase to PI 3-kinase pathway. Oncogene 28: 937-949, 2009.
3. Shiozaki A, Shen-Tu G, Bai X, Iitaka D, De Falco V, Santoro M, Keshavjee S and Liu M: XB130 mediates cancer cell proliferation and survival through multiple signaling events downstream of Akt. PLoS One 7: e43646, 2012.
4. Cho HR, Wang Y, Bai X, Xiang YY, Lu C, Post A, Al Habeeb A and Liu M: XB130 deficiency enhances carcinogen-induced skin tumorigenesis. Carcinogenesis 40: 1363-1375, 2019.
5. Shiozaki A and Liu M: Roles of XB130, a novel adaptor protein, in cancer. J Clin Bioinforma 1: 10, 2011.
6. Wang Q, Yang G, Jiang Y, Luo M, Li C, Zhao Y, Xie Y, Song K and Zhou J: XB130, regulated by miR-203, miR-219, and miR-4782-3p, mediates the proliferation and metastasis of non-small-cell lung cancer cells. Mol Carcinog 59: 557-568, 2020.
7. Song K, Jiang Y, Zhao Y, Xie Y, Zhou J, Yu W and Wang Q: Members of the miR-30 family inhibit the epithelial-to-mesenchymal transition of non-small-cell lung cancer cells by suppressing XB130 expression levels. Oncol Lett 20: 68, 2020.
8. Shi M, Zheng D, Sun L, Wang L, Lin L, Wu Y, Zhou M, Liao W, Liao Y, Zuo Q and Liao W: XB130 promotes proliferation and invasion of gastric cancer cells. J Transl Med 12: 1, 2014.
9. Shi M, Huang W, Lin L, Zheng D, Zuo Q, Wang L, Wang N, Wu Y, Liao Y and Liao W: Silencing of XB130 is associated with both the prognosis and chemosensitivity of gastric cancer. PLoS One 7: e41660, 2012.
10. Shiozaki A, Lodyga M, Bai XH, Nadesalingam J, Oyaizu T, Winer D, Asa SL, Keshavjee S and Liu M: XB130, a novel adaptor protein, promotes thyroid tumor growth. Am J Pathol 178: 391-401, 2011.
11. Mayr C: Evolution and Biological Roles of Alternative 3'UTRs. Trends Cell Biol 26: 227-237, 2016.
12. Khabar KS: Hallmarks of cancer and AU-rich elements. Wiley Interdiscip Rev RNA 8: e1368, 2017.
13. Kovarik P, Ebner F and Sedlyarov V: Posttranscriptional regulation of cytokine expression. Cytokine 89: 21-26, 2017.
14. Vlasova-St Louis I and Bohjanen PR: Feedback regulation of kinase signaling pathways by AREs and GREs. Cells 5: 4, 2016.
15. Barreau C, Paillard L and Osborne HB: AU-rich elements and associated factors: Are there unifying principles? Nucleic Acids Res 33: 7138-7150, 2006.
16. Halees AS, Hitti E, Al-Saif M, Mahmoud L, Vlasova-St Louis IA, Beisang DJ, Bohjanen PR and Khabar K: Global assessment of GU-rich regulatory content and function in the human transcriptome. RNA Biol 8: 681-691, 2011.
17. Vlasova IA, Tahoe NM, Fan D, Larsson O, Rattenbacher B, Sternjohn JR, Vasdewani J, Karypis G, Reilly CS, Bitterman PB and Bohjanen PR: Conserved GU-rich elements mediate mRNA decay by binding to CUG-binding protein 1. Mol Cell 29: 263-270, 2008.
18. Li F, Zhao H, Su M, Xie W, Fang Y, Du Y, Yu Z, Hou L and Tan W: HnRNP-F regulates EMT in bladder cancer by mediating the stabilization of Snail1 mRNA by binding to its 3' UTR. EBioMedicine 45: 208-219, 2019.
19. Zhang R, Zhang J, Wu Q, Meng F and Liu C: XB130: A novel adaptor protein in cancer signal transduction. Biomed Rep 4: 300-306, 2016.
20. Hussain H and Chong NF: Combined overlap extension PCR method for improved site directed mutagenesis. Biomed Res Int 2016: 8041532, 2016.
21. Livak KJ and Schmittgen TD: Analysis of relative gene expression data using real-time quantitative PCR and the 2(-Delta Delta C(T)) method. Methods 25: 402-408, 2001.
22. Tao X and Gao G: Tristetraprolin recruits eukaryotic initiation factor 4E2 To repress translation of AU-Rich element-containing mRNAs. Mol Cell Biol 35: 3921-3932, 2015.
23. Lodyga M, Bai XH, Kapus A and Liu M: Adaptor protein XB130 is a Rac-controlled component of lamellipodia that regulates cell motility and invasion. J Cell Sci 123(Pt 23): 4156-4169, 2010.
24. Moodley S, Hui Bai X, Kapus A, Yang B and Liu M: XB130/Tks5 scaffold protein interaction regulates Src-mediated cell proliferation and survival. Mol Biol Cell 26: 4492-4502, 2015.
25. Shen J, Jin C, Liu Y, Rao H, Liu J and Li J: XB130 enhances invasion and migration of human colorectal cancer cells by promoting epithelial-mesenchymal transition. Mol Med Rep 16: 5592-5598, 2017.
26. Wu Q, Nadesalingam J, Moodley S, Bai X and Liu M: XB130 translocation to microfilamentous structures mediates NNK-induced migration of human bronchial epithelial cells. Oncotarget 6: 180501-180565, 2015.
27. Yamanaka D, Akama T, Chida K, Minami S, Ito K, Hakuno F and Takahashi S: Phosphatidylinositol 3-Kinase-Associated Protein (PI3KAP)/XB130 crosslinks actin filaments through its actin binding and multimerization properties in vitro and enhances endocytosis in HEK293 cells. Front Endocrinol (Lausanne) 7: 89, 2016.
28. Cok SJ and Morrison AR: The 3'-untranslated region of murine cyclooxygenase-2 contains multiple regulatory elements that alter message stability and translational efficiency. J Biol Chem 276: 23179-23185, 2001.
29. Baou M, Jewell A and Murphy JJ: TIS11 family proteins and their roles in posttranscriptional gene regulation. J Biomed Biotechnol 2009: 634520, 2009.
30. Fallmann J, Sedlyarov V, Tanzer A, Kovarik P and Hofacker IL: AREsite2: An enhanced database for the comprehensive investigation of AU/GU/U-rich elements. Nucleic Acids Res 44(D1): D90-D95, 2016.
31. Mukhopadhyay D, Houchen CW, Kennedy S, Dieckgraefe BK and Anant S: Coupled mRNA stabilization and translational silencing of cyclooxygenase-2 by a novel RNA binding protein, CUGBP2. Mol Cell 11: 113-126, 2003.
32. Dean JL, Wait R, Mahtani KR, Sully G, Clark AR and Saklatvala J: The 3' untranslated region of tumor necrosis factor alpha mRNA is a target of the mRNA-stabilizing factor HuR. Mol Cell Biol 21: 721-730, 2001.
33. Raineri I, Wegmueller D, Gross B, Certa U and Moroni C: Roles of AUF1 isoforms, HuR and BRF1 in ARE-dependent mRNA turnover studied by RNA interference. Nucleic Acids Res 32: 1279-1288, 2004.
34. Bakheet T, Williams BR and Khabar KS: ARED 3.0: The large and diverse AU-rich transcriptome. Nucleic Acids Res 34(Database Issue): D111-D114, 2006.
35. Halees AS, El-Badrawi R and Khabar KS: ARED Organism: Expansion of ARED reveals AU-rich element cluster variations between human and mouse. Nucleic Acids Res 36(Database Issue): D137-D140, 2008.
36. Ostareck DH, Ostareck-Lederer A, Wilm M, Thiele BJ, Mann M and Hentze MW: mRNA silencing in erythroid differentiation: hnRNP K and hnRNP E1 regulate 15-lipoxygenase translation from the 3' end. Cell 89: 597-606, 1997.
37. Wang S, Zhang J, Theel S, Barb JJ, Munson PJ and Danner RL: Nitric oxide activation of Erk1/2 regulates the stability and translation of mRNA transcripts containing CU-rich elements. Nucleic Acids Res 34: 3044-3056, 2006.
38. Alcorta-Sevillano N, Macías I, Rodríguez CI and Infante A: Crucial role of Lamin A/C in the migration and differentiation of MSCs in bone. Cells 9: 1330, 2020.
39. Wang Y, Sun Y, Fu Y, Guo X, Long J, Xuan LY, Wei CX and Zhao M: Calumenin relieves cardiac injury by inhibiting ERS-initiated apoptosis during viral myocarditis. Int J Clin Exp Pathol 10: 7277-7284, 2017.
40. Ackermann A and Brieger A: The role of nonerythroid spectrin αII in cancer. J Oncol 2019: 7079604, 2019.
41. Du HQ, Wang Y, Jiang Y, Wang CH, Zhou T, Liu HY and Xiao H: Silencing of the TPM1 gene induces radioresistance of glioma U251 cells. Oncol Rep 33: 2807-2814, 2015.
42. Vedeler A, Hollås H, Grindheim AK and Raddum AM: Multiple roles of annexin A2 in post-transcriptional regulation of gene expression. Curr Protein Pept Sci 13: 401-412, 2012.
43. Cheng L and Tong Q: Interaction of FLNA and ANXA2 promotes gefitinib resistance by activating the Wnt pathway in non-small-cell lung cancer. Mol Cell Biochem 476: 3563-3575, 2021.
44. Cooke A, Schwarzl T, Huppertz I, Kramer G, Mantas P, Alleaume AM, Huber W, Krijgsveld J and Hentze MW: The RNA-Binding Protein YBX3 controls amino acid levels by regulating SLC mRNA abundance. Cell Rep 27: 3097-3106.e5, 2019.